

Published in IET Communications
 Received on 15th November 2008
 Revised on 10th June 2009
 doi: 10.1049/iet-com.2008.0658



Promising performance of a frequency-modulated differential chaos shift keying ultra-wideband system under indoor environments

X. Min¹ W. Xu¹ L. Wang¹ G. Chen²

¹Department of Communication Engineering, Xiamen University, Fujian, People's Republic of China

²Department of Electronic Engineering, City University of Hong Kong, Hong Kong SAR, People's Republic of China
 E-mail: wanglin@xmu.edu.cn

Abstract: In this study, the performance of the frequency-modulated differential chaos shift keying (FM-DCSK) ultra-wideband (UWB) system is evaluated through two important system parameters, the guard interval and the integration interval of the integrator, over indoor communication channels. It is found that the existing FM-DCSK UWB system suffers severe performance degradation in the IEEE 802.15.4a low-rate application. To resolve this problem, a new optimising scheme for the integration interval is presented. Simulation results show that the performance of the proposed scheme is significantly improved and becomes insensitive to the data rate. In addition, some notable advantages are evident in the proposed system, such as moderate multiple-access capability and feasible cross-layer optimisation.

1 Introduction

Ultra-wideband (UWB) transmission has received great attention in both academia and industry for its promising applications in wireless communications, especially in wireless personal area networks (WPAN). A UWB signal has a wide bandwidth, which is either greater than 500 MHz or more than 20% of its centre frequency, and can be extended from 3.1 up to 10.6 GHz [1].

In recent years, several chaotic modulation schemes have been proposed as candidates of the UWB radio standards for WPAN by the IEEE 802.15.4a Task Group [2–4], because chaotic signals have numerous advantages [5]. First, with its inherent wideband and low cross-correlation properties, it resists multipath fading prominently. Second, it offers a cheap alternative solution to spreading signals generated by conventional spread-spectrum techniques. Third, the special spectral properties of chaotic signals can be controlled so as to satisfy the Federal Communications Commission regulations. Last but not the least, it can be easily generated by simple

circuits. Among all the chaotic modulation schemes, frequency-modulated differential chaos shift keying (FM-DCSK) is proven not only having the best noise performance but also achieving an excellent anti-multipath fading capability [6–11]. Meanwhile, as a transmitted reference (TR) system, FM-DCSK has preferable TR system's advantages (e.g. no need of channel estimation, no crucial requirement of exact synchronisation and only need frame or symbol rate sampling). Consequently, it has been considered as a feasible scheme for UWB transmission and a good candidate for WPAN, especially for low complexity and low data-rate applications. An explicit expression for noise performance was given over additive white Gaussian noise (AWGN) channels [12]. As one promising candidate, an FM-DCSK UWB radio system was demonstrated recently [5].

To adapt to UWB dense multipath channels, the original FM-DCSK scheme is modified in the FM-DCSK UWB system. In the transmitter, null signals as the guard interval of anti-interference are inserted in between the reference and the information signals. And in the receiver, the

integration interval of the correlative integrator is worthy of attention. Since the non-coherent FM-DCSK scheme belongs to a TR system, the integration length of the integrator in the receiver determines how much signal energy and noise energy will be captured, which significantly affects the system performance especially in the UWB dense multipath channels [13]. Clearly, the guard interval and the integration interval of the integrator are two important parameters of the FM-DCSK UWB system. These two parameters, however, have not been carefully considered in the published literatures on FM-DCSK UWB system [5, 12].

On the other hand, for conventional TR-UWB systems based on monocyclic pulse, many works on analysis and optimisation about the guard interval and the integration interval have been reported [13–16]. In particular, a recent paper [17] has performed theoretical analysis of the integration interval for the TR-UWB system and presented a method of synchronising and optimising the integration interval, which can estimate the optimal integration interval through the received training signals. However, unlike the conventional TR-UWB system with fixed waveforms, the carriers in the FM-DCSK UWB system are continuously varying chaotic waveforms, that is, the chaotic carriers are not the same in different symbols. And the carriers of different symbols have low cross-correlation values, thanks to the special properties of chaotic signals. Thus, the method using the idea of inter-symbol correlations proposed in [17] is in general not applicable to the FM-DCSK UWB system.

In this paper, the main focus is on optimising two key parameters and considering the feasibility of the IEEE 802.15.4a low-rate application of the FM-DCSK UWB system. Its bit error rate (BER) analysis will be performed, and a mathematical expression of the optimal integration interval will be given. A new scheme for optimising the integration interval will be developed by manipulating the correlation between the chaotic reference signal and its delayed template. This can resolve the performance deterioration problem of the existing FM-DCSK UWB system appeared in the 802.15.4a low-rate application. Both the problem of existing system and the efficacy of new scheme will be revealed through simulations. Finally, some other benefits of the proposed scheme will be discussed, which are useful for enhancing the new FM-DCSK UWB system.

2 System model of FM-DCSK UWB

2.1 UWB channel model

A typical measurement-based UWB channel model [18] was adopted by the IEEE 802.15.4a. This model is valid from 2 to 10 GHz frequency range and under several different environments including the indoor residential, indoor office, outdoor, industrial and open-outdoor environments under both line-of sight (LOS) and non-LOS (NLOS)

scenarios. A total of nine channel models (i.e. CM1–CM9) are defined, as listed in Table 1.

2.2 System structure

The FM-DCSK UWB system model is illustrated in Fig. 1. As can be seen, the structure of the FM-DCSK UWB system is not much different from the original FM-DCSK scheme, but the form of its signals has been changed to be in an UWB format in the transmitter, which contains null signals during the bit duration.

2.2.1 First key parameter: guard interval: In the FM-DCSK UWB scheme, it uses two signals as carriers, called reference and information chips, respectively. The signal structure of the FM-DCSK UWB is illustrated in Fig. 2, where T_f is the bit duration, T_s is the duration of the chips and T_g is the guard interval duration between the reference and the information chips. Their relations and the data rate R of the system can be expressed as

$$T_g = \frac{(T_f - 2T_s)}{2}, \quad R = \frac{1}{T_f} = \frac{1}{2(T_g + T_s)} \quad (1)$$

Table 1 IEEE 802.15.4a channel model

Mode	Environment	Bandwidth (GHz)
CM1	residential LOS	2–10
CM2	residential NLOS	2–10
CM3	office LOS	3–6
CM4	office NLOS	3–6
CM5	outdoor LOS	3–6
CM6	outdoor NLOS	3–6
CM7	industrial LOS	2–8
CM8	industrial NLOS	2–8
CM9	open outdoor NLOS	2–8

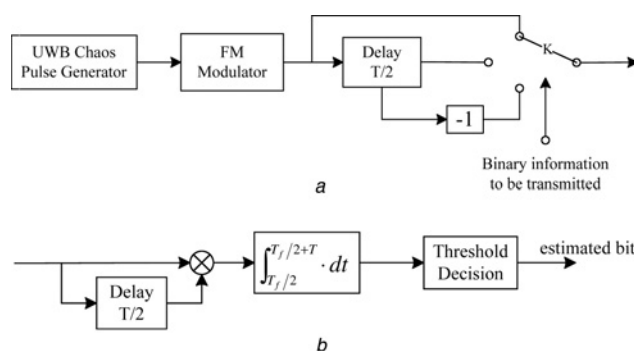


Figure 1 Block diagram of the FM-DCSK UWB system

a Transmitter
b Receiver

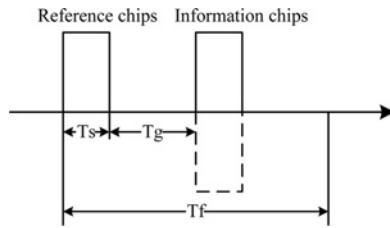


Figure 2 Signal structure of the FM-DCSK UWB system

It can be seen from (1) that the data rate R solely depends on the guard interval duration T_g when T_s is constant. Thus, one can control the data rate by regulating T_g . This issue will be further discussed in Section 4.

2.2.2 Second key parameter: integration interval:

In the receiver end, a correlator and a threshold detector are used to estimate the information bits. Considering the integration interval T of the correlator, it is determined to be $T_f/2$ in the original FM-DCSK system over an arbitrary transmission channel [6] or to be T_s in the FM-DCSK UWB system over the AWGN channel [12]. The transmission over a typical UWB channel leads to multipath propagation, so the integration interval T will no longer be $T_f/2$ or T_s , but becomes a changeable value in between T_s and $T_f/2$. Using a shorter integration interval, the receiver can only capture a small fraction of the desired signal energy, whereas unnecessary noise energy will be accumulated at the receiver on a longer integration interval [13]. Therefore the integration interval of the FM-DCSK UWB system must be carefully selected in the indoor UWB applications.

3 Analysis and optimisation of system performance

3.1 Theoretical analysis of BER

By inserting adequate null signals between the reference and the information pulse, the inter-pulse interference and the inter-symbol interference (ISI) can be completely avoided, if the last trivial part of the channel impulse response is ignored. Thus, the tasks of demodulation and detection of the proposed system can be carried out symbol by symbol.

In the transmitter, the modulated signal is

$$s(t) = \sqrt{\frac{E_b}{2}} [c(t) + ac(t - T_f/2)] \quad (2)$$

where E_b is the signal energy per bit, $c(t)$ is the frequency-modulated chaotic pulse and $\int_0^{T_f} c^2(t) dt = 1$, $a \in \{-1, +1\}$ is the binary input and T_f is the bit duration.

The IEEE 802.15.4a channel model can be generalised by a quasi-static tapped delay line [18]. That is

$$h(t) = \sum_{l=1}^L \alpha_l \delta(t - \tau_l) \quad (3)$$

where L is the total number of multipath taps, α_l and τ_l are the complex-valued gain and delay of the l th tap, respectively. Here $\sum_{l=1}^L \alpha_l^2 = 1$.

In the absence of ISI, the received signal is

$$r(t) = \sqrt{\frac{E_b}{2}} [g(t) + ag(t - T_f/2)] + n(t) \quad (4)$$

where $g(t) = c(t) \otimes h(t)$, \otimes is the operator of convolution and $n(t)$ is the zero-mean additive complex-valued Gaussian noise with variance N_0 .

Suppose that a data symbol $a = 1$ is transmitted, so the output of the detector correlator is

$$y = \Re \left\{ \int_{T_f/2}^{T_f/2+T} r(t - T_f/2) r^*(t) dt \right\} \quad (5)$$

Substituting (4) into (5), it can be obtained as

$$\begin{aligned} y = & \frac{E_b}{2} \int_{T_f/2}^{T_f/2+T} |g(t - T_f/2)|^2 dt \\ & + \sqrt{\frac{E_b}{2}} \int_{T_f/2}^{T_f/2+T} \Re\{g(t - T_f/2)n^*(t)\} dt \\ & + \sqrt{\frac{E_b}{2}} \int_{T_f/2}^{T_f/2+T} \Re\{g^*(t - T_f/2)n(t - T_f/2)\} dt \\ & + \int_{T_f/2}^{T_f/2+T} \Re\{n(t - T_f/2)n^*(t)\} dt \end{aligned} \quad (6)$$

$$y = \zeta_1 + \zeta_2 + \zeta_3 + \zeta_4 \quad (7)$$

where the superscript $*$ denotes complex conjugate, $\Re\{x\}$ takes the real part of x , T is the integration time of the correlator, ζ_1 is the signal energy captured in the integration, ζ_2 and ζ_3 are the 'signal cross noise' terms and ζ_4 is the 'noise cross noise' term.

When $T_f \gg 2T_s$, in terms of the conclusion on the TR-UWB systems [19], these three terms can be approximately considered as independent Gaussian random variables. Their distributions are, respectively

$$\zeta_2, \zeta_3 \sim N\left(0, \frac{N_0 E_b \int_0^T |g(t)|^2 dt}{4}\right) \quad (8)$$

$$\zeta_4 \sim N(0, N_0^2 BT) \quad (9)$$

where B is the bandwidth of $n(t)$ or equivalently the bandwidth of the system. Hence, the BER probability can be written as

$$P_e = P(y < 0) = P(\zeta_1 + \zeta_2 + \zeta_3 + \zeta_4 < 0) = Q \left\{ \sqrt{\frac{(E_b \int_0^T |g(t)|^2 dt)^2}{4N_0^2 BT + 2N_0 E_b \int_0^T |g(t)|^2 dt}} \right\} \quad (10)$$

where $Q(x) \simeq 1/\sqrt{2\pi} \int_x^\infty e^{-t^2/2} dt$ is a decreasing function. Consequently, the optimisation T_{opt} of the integration interval is equivalent to the maximisation

$$T_{opt} = \arg \max_T \frac{(E_b \int_0^T |g(t)|^2 dt)^2}{4N_0^2 BT + 2N_0 E_b \int_0^T |g(t)|^2 dt} \quad (11)$$

Equation (11) not only proves the existence of the optimal integration interval T_{opt} , but also shows that the optimal value depends on E_b , N_0 , B and $g(t)$. For the proposed FM-DCSK scheme, the bandwidth B and the bit energy E_b are both constant [6]. Thus, the optimal integration interval depends on the N_0 (i.e. E_b/N_0 when E_b is constant) and the channel conditions here. Using (11), one can search for an optimal integration interval T_{opt} through computer computation. However, note that $g(t)$ in (11) is the ideal noise-free received signal. As obtaining $g(t)$ through the received signal $r(t)$ is relatively difficult in practice, the estimation of T_{opt} should be implemented by a simple and feasible method, corresponding to the low-cost and low-power applications. The alternative method will be further discussed in the next section.

3.2 An optimisation scheme for the integration interval

As above, when a data symbol $a = 1$ is transmitted, the error probability can be written as $P_e = P(\zeta_1 + \zeta_2 + \zeta_3 + \zeta_4 < 0)$. For a function $X(T) = \zeta_1 + \zeta_2 + \zeta_3 + \zeta_4$, P_e is equal to $P(X(T) < 0)$ and decreases with $X(T)$. Therefore corresponding to the minimum error probability P_{emin} , the optimal integration interval T_{opt} is equivalent to the maximisation

$$T_{opt} = \arg \max_T (X(T)) \quad (12)$$

Since $X(T)$ is precisely the output of the detector-correlator, T_{opt} can be found by searching in the correlation results based on (12). Considering the continuously varying carrier in the FM-DCSK UWB system, a new optimisation scheme of integration interval is proposed. Its block diagram is shown in Fig. 3. Two cases (i.e. single-user and multiple-user case) will be described, respectively.

3.2.1 Single-user case: Comparing between Figs. 1a and 3a, two blocks D1 and π are added in the proposed

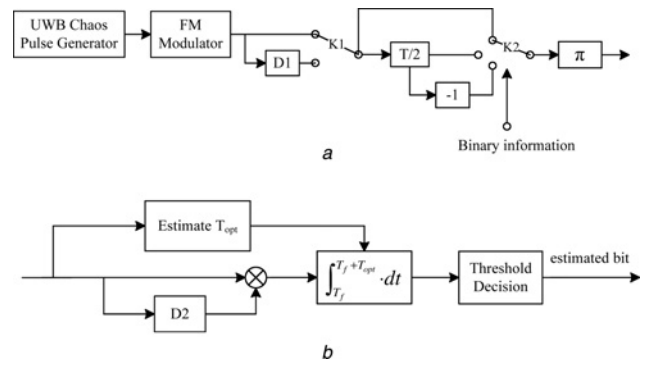


Figure 3 Block diagram of the proposed optimisation FM-DCSK UWB system

a Transmitter
b Receiver

transmitter. Here, D1 is a delay unit and π is an interleaver. The function of D1 is making the first bit reference pulse delay one-bit duration T_f at the beginning of each frame signal. Therefore the reference pulse of the second bit is even the delay version of the first one, that is, they are the same actually. Here, switch K1 holds on above unless during the second bit duration per-frame. The structure of the FM-DCSK modulated signal is shown in Fig. 4a.

As in Fig. 3a, the modulated signals will get through an interleaver π before being transmitted. Here, regular interleaving is performed to make the reference chips of the first bit signal (R1) and the reference chips of the second bit signal (R2) ‘adjacent’. Other bit signals are operated in the same way to make the spaces between reference and relative information chips identical for all bits. The process is shown in Fig. 4b.

In the receiver, comparing between Figs. 1b and 3b, the block named ‘Estimate T_{opt} ’ is new. There are two manipulations herein. First, compute the cross-correlation

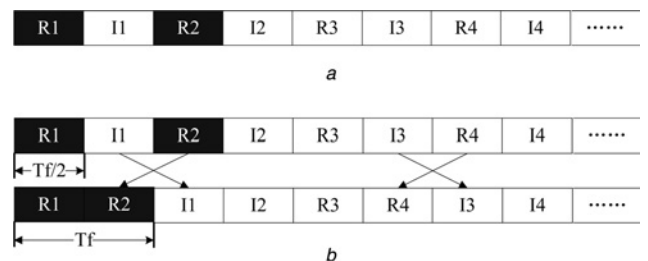


Figure 4 Transmitted signal in the single-user case

a The structure of the modulated signal, where R_i indicates the reference chip and I_i indicates the information chip of the i th bit signal ($i = 1, 2, 3, \dots, N$, N is the bit number per-frame). R2 is the delayed version of R1, so the first two bits have the same reference pulse. The shadow shows that R1 and R2 are the same actually

b Regular interleaving is performed in the middle of every two bits

$R_{R1,R2}(t)$ between R1 and R2. Second, through searching, find appropriate integration interval T_{opt} corresponding to the largest cross-correlation value.

Considering D2 in Fig. 3b, the relevant delay is $T_f/2$ in the original scheme as in Fig. 1b. But as interleaving in the transmitter, the information chips (I_i) is delayed away from the relevant reference chips (R_i) not by the original half-bit ($T_f/2$) but one bit duration (T_f) in the proposed scheme, shown in Fig. 4b. Therefore the delay of D2 should be T_f instead of $T_f/2$. Naturally, the initial point of the integration in the integrator is changed to T_f , also shown in Fig. 3b.

3.2.2 Multiple-user case: Considering the interleaving process in Fig. 4b again, the spaces between reference chips and relevant information chips are doubled by one time interleaving in the above single-user case. Suppose increasing the times of interleaving, the delays between reference and information chips will become larger. As shown in Fig. 5a, if the regular interleaving is performed again in the middle of every four bits, the delays between reference and information chips will be added to $2T_f$. This may provide a simple alternative solution to multiple-access communications. Since the delays between reference and information chips are equal to $2^{k-1}T_f$, here k is the times of interleaving, corresponding to k th user. Thus, different delays of different users will be achieved through different times interleaving. Based on the low cross correlation of chaotic signals, one can distinguish users by different delays between the reference and the relevant information chips [20].

When compared with the single-user case, the potential multiple-user scheme is easy to implement without any compensatory measures in the proposed optimisation

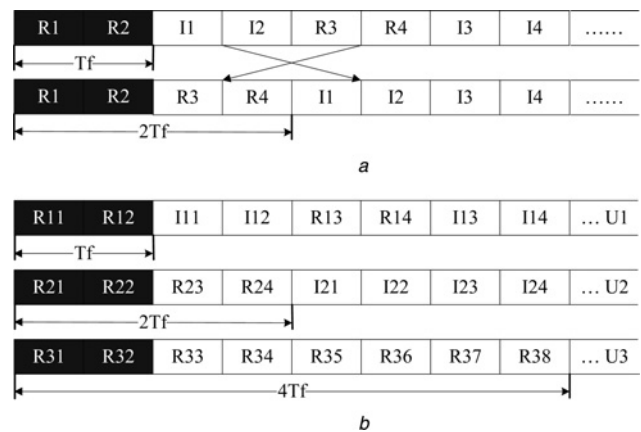


Figure 5 Transmitted signal in the multiple-user case
 a Regular interleaving is performed again in the middle of every four bits
 b An example with three users where the delays between reference and information chips are T_f , $2T_f$ and $4T_f$, respectively, for user one (U1), user two (U2) and user three (U3). The optimisation of integration interval is still implemented by R_{i1} and R_{i2} (shaded) for i th user

mechanism. In the transmitter as in Fig. 3a, the times of the interleaving in π are distinguishing for different users. To the receiver shown in Fig. 3b, the difference is from the delays in the block D2, that is, different delays of different users between reference and information chips. It is noted that the estimation of T_{opt} is performed by correlating R_{i1} and R_{i2} in the 'estimate T_{opt} ' module and is identical for all users.

4 Simulation results

The simulations shown below are performed under indoor environments of the IEEE 802.15.4a channel [17], which

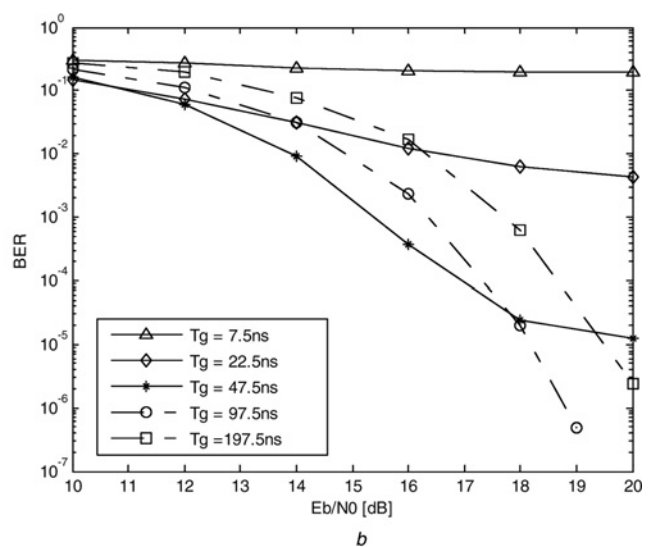
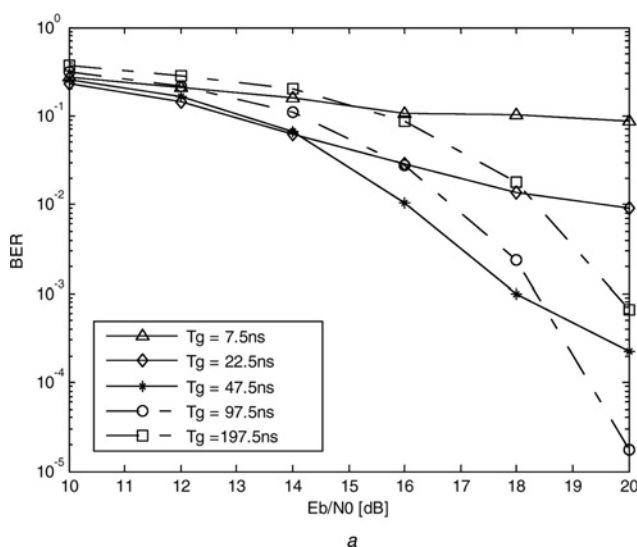


Figure 6 Performance of the FM-DCSK UWB system with non-optimised integration interval $T = T_f/2$ when the guard interval length T_g is 7.5, 22.5, 47.5, 97.5 and 197.5 ns

a CM1

b CM4

The figures of CM2 and CM3 are omitted because they are similar to CM1 and CM4

are based on LOS indoor residential (CM1), NLOS indoor residential (CM2), LOS indoor office environments (CM3) and NLOS indoor office environments (CM4), respectively. It is assumed that the channel impulse response is invariant in the frame duration with 100 bits. And the bandwidth B is set to 500 MHz in all the following simulations.

4.1 Guard interval

In this subsection, the BER performance of the FM-DCSK UWB system is evaluated through the guard interval. In general, a proper duration should be well trade-off between the BER performance and the data rate.

Firstly, we use half-bit duration $T_f/2$ as the integration interval, non-optimised as in the original FM-DCSK scheme, and fix the chips duration T_s to 2.5 ns. Fig. 6 shows the BER performance against T_g (i.e. $T_g = 7.5, 22.5, 47.5, 97.5$ and 197.5 ns) in CM1 and CM4. The BER performance is significantly affected by the guard interval duration T_g . Specifically, it is improved from $T_g = 7.5$ to 47.5 ns, then starts to degrade gradually as T_g increases, and best performance occurs at $T_g = 47.5$ ns (low SNR) or 97.5 ns (high SNR) in CM1 and CM4. Since $T_f = 2(T_s + T_g)$, the increase of T_g means increasing the bit duration T_f when T_s is constant. Thus, with T_g increases, the ISI declines whereas the noise increases because the integration interval is equal to $T_f/2$. Notably, the BER performance is determined by both noise and ISI under such

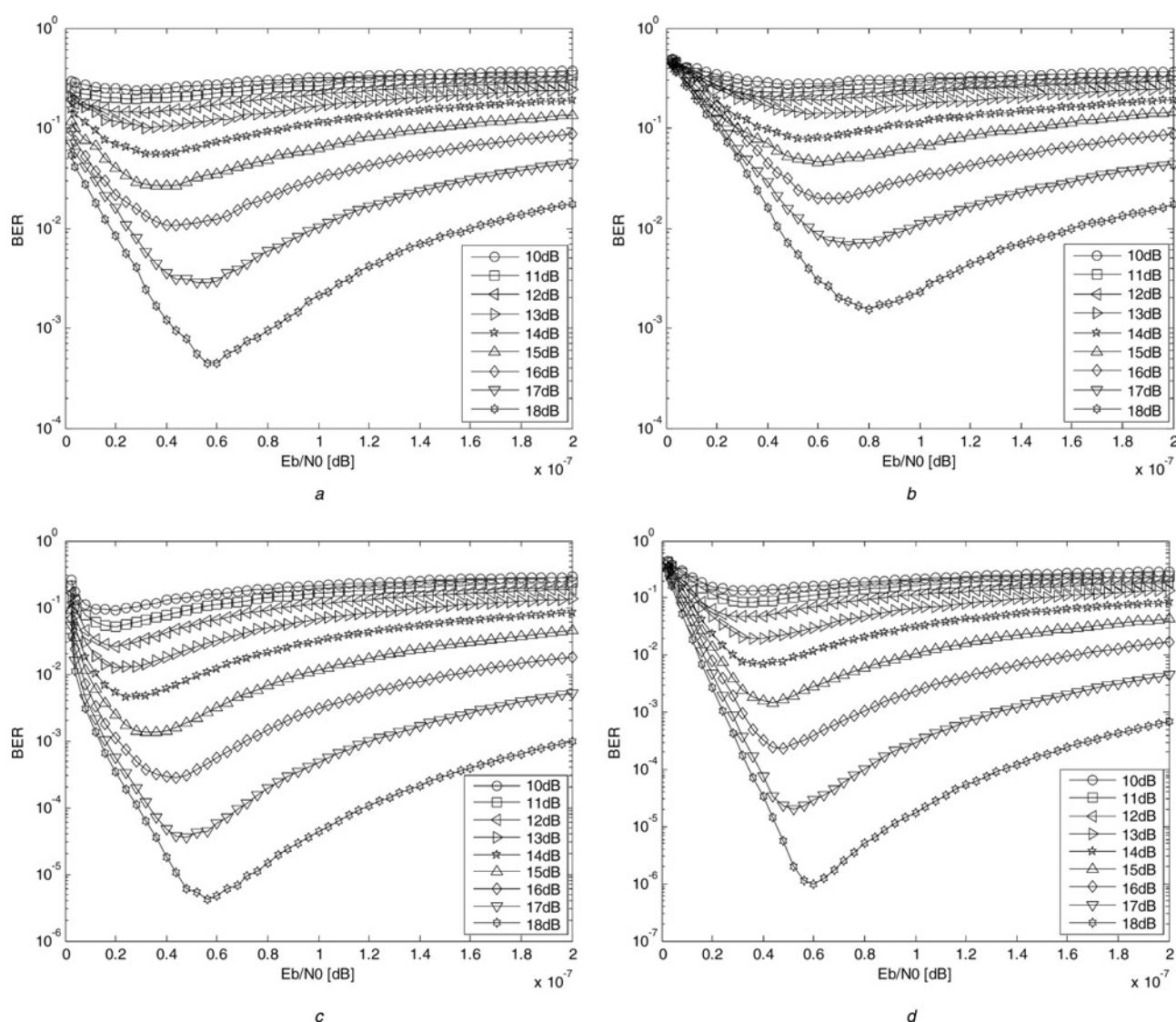


Figure 7 BER as a function of the integration interval, as E_b/N_0 increases from 10 to 18 dB in

- a CM1
- b CM2
- c CM3
- d CM4

circumstances. When T_g is relatively small (e.g. less than 47.5 ns), the advantage of weakening ISI is superior to the disadvantage of increasing noise, therefore the BER performance is improved as T_g increases, as shown in Fig. 6, when T_g is increased from 7.5 to 47.5 ns. However, when T_g is added to a certain value (e.g. $T_g = 97.5$ ns), ISI is unobvious therefore can be negligible. So, the benefit of weakening ISI is inferior to the adverse effect of increasing

noise, when increasing T_g . And, consequently, the performance is degraded, as shown in Fig. 6, when T_g is increased from 97.5 to 197.5 ns.

The above results reveal a serious problem for low-rate applications of the FM-DCSK UWB system. That is when the integration interval is the original half-bit duration, BER performance suffers deterioration as the guard interval

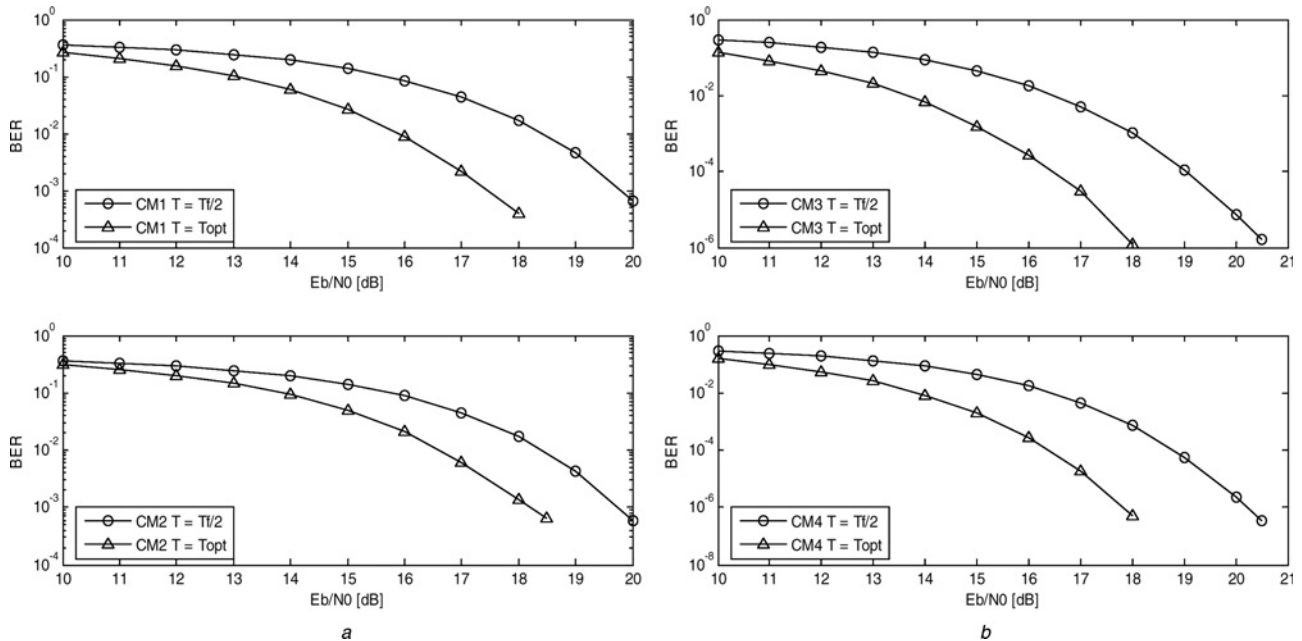


Figure 8 Performance comparison between the original FM-DCSK UWB scheme ($T = T_f/2$) and the optimisation scheme ($T = T_{opt}$) with data rate at 2.5 Mbps in

a CM1 and CM2
b CM3 and CM4

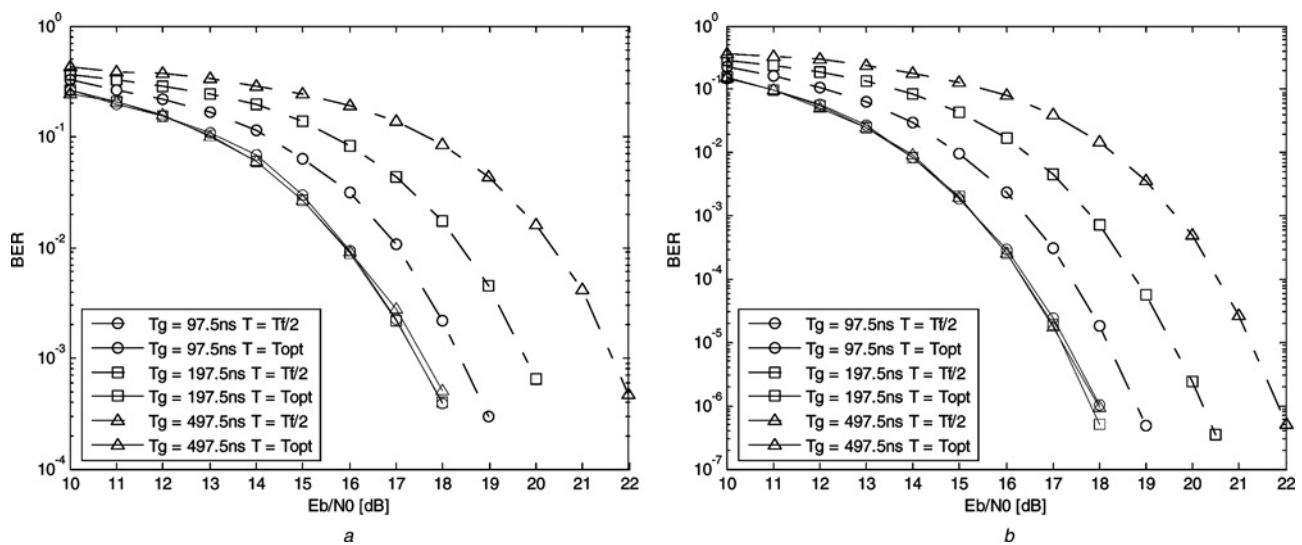


Figure 9 Performance comparison between the original FM-DCSK UWB scheme ($T = T_f/2$) and the optimisation scheme ($T = T_{opt}$) with data rates at 5 Mbps ($T_g = 97.5$ ns), 2.5 Mbps ($T_g = 197.5$ ns) and 1 Mbps ($T_g = 497.5$ ns) in

a CM1
b CM4

increases (i.e. the data rate lowers), especially in the absence of ISI. Thus, the optimisation of integration interval must be considered, which is further investigated below.

4.2 Integration interval

This subsection considers the influence of the integration interval on the system performance. BER performance of the existing FM-DCSK UWB system is simulated with different integration intervals T_i , while fixing the guard interval duration T_g . In order to avoid ISI better, T_g is set as 197.5 ns and T_s remains at 2.5 ns. Fig. 7 shows the BER performance as a function of the integration interval T (from $T_s = 2.5$ ns to $T_i/2 = 200$ ns) in the different E_b/N_0 and different channel modes case. It is clear that there exists an optimal integration interval when BER is minimised in the curve corresponding to each E_b/N_0 . Notice that in CM1–CM4, the optimal value of T is within 25–60, 40–80, 20–60 and 30–60 ns, respectively, depending on E_b/N_0 . The simulation results prove the issue analysed in Section 3 that the optimal integration interval depends on the channel mode and E_b/N_0 .

4.3 Performance of the optimisation scheme

In this subsection, the BER performance of the proposed optimisation scheme is simulated over indoor channels from CM1 to CM4.

As in the previous subsection, T_g is set as 197.5 ns and T_s is 2.5 ns (i.e. $R = 2.5$ Mbps). Above simulations have shown that the optimal value of T is within 25–60, 40–80, 20–60 and 30–60 ns, respectively, in CM1–CM4, while E_b/N_0 is from 10 to 18 dB. Accordingly, the searching range of the optimisation scheme is reduced to coincide with the above

results under the same E_b/N_0 to save time and energy. Fig. 8 shows that the BER performance of the optimisation method outperforms the original scheme with the fixed integration interval $T_i/2$ about 2.2 dB when $\text{BER} = 10^{-3}$ in CM1, and similarity in CM3 and CM4 corresponding $\text{BER} = 10^{-5}$, but only about 1.2 dB in CM2 when $\text{BER} = 10^{-3}$. That is because larger excess delays exist in CM2 than the others.

Now, the BER performance of the presented optimisation scheme is evaluated with different guard interval duration $T_g = 97.5, 197.5$ and 497.5 ns, which means data rates R is 5, 2.5 and 1 Mbps, respectively. Other parameters are the same as above. In Fig. 9, when achieving $\text{BER} = 10^{-3}$ in CM1 and $\text{BER} = 10^{-6}$ in CM4, the E_b/N_0 requirement of the optimisation scheme is less than the original scheme about 1, 2.5 and 4.5 when the data rates are 5, 2.5 and 1 Mbps, respectively. It means that the performance gain is increased as the data rate decreases. Similar results are obtained in other two indoor channels, CM2 and CM3. That is because longer bit duration means more unwanted noise energy captured by the non-optimised scheme. Consequently, the optimisation scheme is more effective for low-rate applications.

Considering the non-optimised scheme (dash-dot curves in Fig. 9), its BER performance is affected obviously by the data rate R , and suffers about 3 dB deteriorations when R is decreased from 5 to 1 Mbps. The result is not welcomed by the IEEE 802.15.4a low-rate application with data rates at 1–2 Mbps. Notably, Fig. 9 also shows that the BER performances of the optimised scheme (solid curves) are close to each other even in different data rates $R = 5, 2.5$ and 1 Mbps. In other words, the BER performance optimised by integration interval is no longer sensitive to

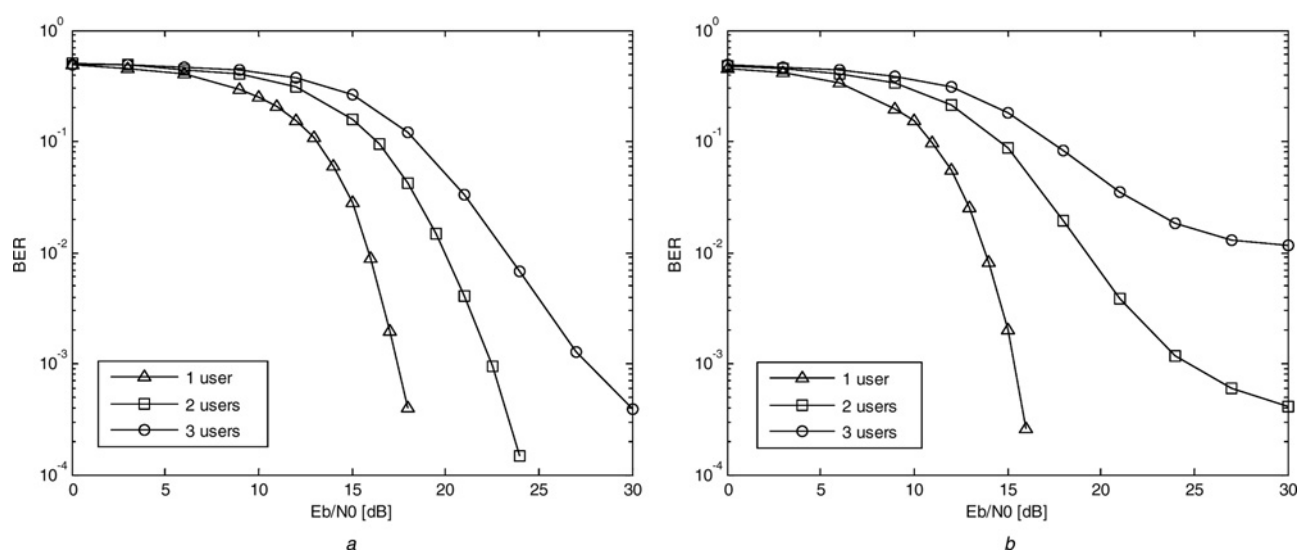


Figure 10 BER against E_b/N_0 for the proposed FM-DCSK UWB system

a CM1
b CM4

the guard interval or the data rate. Therefore the performance deteriorations problem existing in the non-optimised scheme has been resolved effectively.

On the other hand, the importance of the guard interval may not be overlooked in the proposed optimisation scheme. It has been indicated that the data rate can be controlled only by adjusting the guard interval duration T_g , but not regulating the chaotic pulse duration T_s . Since the optimised performance is not sensitive to the data rate R , R can be regulated flexibly by T_g according to the system throughput demand and the network congestion condition, while the point-to-point BER performance is almost unchanged. Thus, cross-layer optimisation is feasible in the wireless network based on the proposed system, using the physical-layer parameter data rate R .

Next, assuming that the required delay can be well achieved, the multiple-access capacity derived from the optimisation scheme is evaluated with data rate $R = 2.5$ Mbps and three users. Each user uses a different chaotic map (User1 uses the cubic map, User2 uses the logistic map and User3 uses the Bernoulli-shift map). Fig. 10 indicates that the proposed system indeed has primary capacity of multiple-access communication. However, it is degraded seriously as the number of users increase both in CM1 and CM4. Similar conclusions are found in CM2 and CM3 through simulations.

In summary, both in theory and simulations, multi-user identification ability is prominent in the proposed system. It is noted that the performance of the multiple-access scheme is not so well, mainly due to noise and multipath, which disturb the correlation property of the received chaotic signals. In the future, some effective measures may be employed to further enhance multiple-access capacity of the proposed system, such as utilising orthogonal codes [21].

5 Conclusions

Two important system parameters (i.e. the guard interval and the integration interval) have been carefully investigated through theoretic analysis and performance simulations over indoor UWB transmission channels. Simulations have revealed a problem that the existing FM-DCSK UWB system suffers serious performance deterioration in the IEEE 802.15.4a low-rate application, for example, about 3 dB attenuations when the data rate is decreased from 5 to 1 Mbps. To overcome this application hurdle, a novel mechanism for optimising the integration interval has been presented. It has been shown that the performance of the new optimisation scheme not only can be greatly improved, about 4 dB gains when the data rate is 1 Mbps, but also become insensitive to the data rate. Accordingly, a new cross-layer optimisation scheme has been presented since the network capacity can be controlled by a physical-layer parameter (i.e. the data rate), which does not affect the point-to-point BER performance. Furthermore, it has been

confirmed that the proposed system can achieve limited multiple-access communication by itself, which can be further improved by some effective measures if needed. Enhanced by these additional superiorities, the optimised FM-DCSK UWB system is believed to be a good candidate for the IEEE 802.15.4a low data-rate application.

6 Acknowledgments

This research was partially supported by the City University of Hong Kong under the SRG Grant 7002274, NSF of China (No. 60272005), NSF of Fujian Province (No. 2008J0035), as well as a Key Project of Science and Technology in the Fujian Province (No. 2006H0039).

7 References

- [1] YANG L.Q., GIANNAKIS G.B.: 'Ultra-wideband communications: an idea whose time has come', *IEEE Signal Proc. Mag.*, 2004, **21**, pp. 26–54
- [2] KIM Y.H., KIM J.H., CHONG C.C., YONG S.K.: 'Chaotic UWB system', Available at: <http://grouper.ieee.org/groups/802/15/pub/05/15-05-0132-03-004a-merged-proposal-chaotic-uwb-system-802-15-4a.pdf>, accessed March 2005
- [3] CHONG C.C., YONG S.K., KIM Y.H., ET AL.: 'Samsung electronics (SAIT) CFP presentation for IEEE 802.15.4a alternative PHY', IEEE 802.15-05-0030-02-004a, 2005
- [4] LEE H.S., LEE C.H., PARK D.J., ET AL.: 'Chaotic pulse based communication system proposal', IEEE 802.15-05-0010-04-004a, 2005
- [5] YONG S.K., CHONG C.C., KOLUMBÁN G.: 'Non-coherent UWB radio for low-rate WPAN applications: a chaotic approach', *Int. J. Wirel. Inf. Netw.*, 2007, **2**, pp. 121–131
- [6] KOLUMBÁN G., KENNEDY M.P., KIS G., JÁKÓ Z.: 'FM-DCSK: a novel method for chaotic communications'. Proc. IEEE Int. Symp. Circuits and Systems, Monterey, CA, USA, May 1998, pp. 477–480
- [7] KENNEDY M.P., KOLUMBÁN G., KIS G., JÁKÓ Z.: 'Performance evaluation of FM-DCSK modulation in multipath environments', *IEEE Trans. Circuits Syst.-I*, 2000, **47**, (12), pp. 1702–1711
- [8] KOLUMBÁN G., KENNEDY M.P., KIS G., JÁKÓ Z.: 'Chaotic communications with correlator receivers: theory and performance limits', *Proc. IEEE*, 2002, **90**, (5), pp. 711–732
- [9] YE L.F., CHEN G., WANG L.: 'Essence and advantages of FM-DCSK technique versus conventional spread-spectrum communication methods', *Circuits, Syst. Signal Process*, 2005, **5**, pp. 657–673

- [10] WANG L., ZHANG C., CHEN G.: 'Performance of an SIMO FM-DCSK Communication System', *IEEE Trans. Circuits Syst.-II*, 2008, **55**, (5), pp. 457–461
- [11] XIA Y.X., TSE C.K., LAU F.C.M., KOLUMBÁN G.: 'Performance of frequency-modulated differential-chaos-shift-keying communication system over multipath fading channels with delay spread', *Int. J. Bifurcation Chaos.*, 2005, **15**, (12), pp. 4027–4033
- [12] KOLUMBÁN G.: 'UWB technology: chaotic communications versus noncoherent impulse radio'. Proc. European Conf. Circuit Theory and Design, Cork, Ireland, August 2005, vol. 2, pp. 79–82
- [13] NAY, SAQUIB M.: 'Analysis of the channel energy capture in ultra-wideband transmitted reference systems', *IEEE Trans. Commun.*, 2007, **55**, (2), pp. 262–265
- [14] FRANZ S., MITRA U.: 'Integration interval optimization and performance analysis for UWB transmitted reference systems'. Proc. Joint UWBST&IWUWBS, Kyoto, Japan, May 2004, pp. 26–30
- [15] CHAO Y.L.: 'Optimal integration time for UWB transmitted reference correlation receivers'. Proc. Conf. Signals, Systems and Computers, Pacific Grove, CA, USA, November 2004, vol. 1, pp. 647–651
- [16] ROMME J., WITRISAL K.: 'Transmitted-reference UWB systems using weighted autocorrelation receivers', *IEEE Trans. Microw. Theory Tech.*, 2006, **54**, (4), pp. 1754–1761
- [17] ZHANG R.R., DONG X.D.: 'Synchronization and integration region optimization for UWB signals with non-coherent detection and auto-correlation detection', *IEEE Trans. Commun.*, 2008, **56**, (5), pp. 790–798
- [18] Channel Model Subcommittee: 'Status of models for UWB propagation channel, IEEE 802.15.4a channel model (final report)', 2004
- [19] CHAO Y.L., SCHOLTZ R.A.: 'Optimal and suboptimal receivers for ultra wideband transmitted reference systems'. Proc. IEEE Global Telecommunications Conf., San Francisco, USA, December 2003, vol. 2, pp. 759–763
- [20] LAU F.C.M., YIP M.M., TSE C.K., HAO S.F.: 'A multiple-access technique for differential chaos-shift keying', *IEEE Trans. Circuits Syst.-I*, 2002, **49**, (1), pp. 96–104
- [21] LI H., DAI X.C., XU P.X.: 'A CDMA based multiple-access scheme for DCSK'. Proc. IEEE Int. Symp. Circuits and Systems, Vancouver, British Columbia, Canada, May, 2004, vol. 1, pp. 313–316